

## THE NON-RADIAL PROPAGATION OF CORONAL STREAMERS WITHIN A SOLAR CYCLE

This article has been downloaded from IOPscience. Please scroll down to see the full text article.

2010 ApJ 714 805

(<http://iopscience.iop.org/0004-637X/714/1/805>)

[The Table of Contents](#) and [more related content](#) is available

Download details:

IP Address: 195.201.30.101

The article was downloaded on 15/04/2010 at 02:29

Please note that [terms and conditions apply](#).

## THE NON-RADIAL PROPAGATION OF CORONAL STREAMERS WITHIN A SOLAR CYCLE

A. G. TLATOV

Kislovodsk Mountain Station, The Central Astronomical Observatory of RAS at Pulkovo, 357700, Box-145, Ggarina St., 100, Kislovodsk, Russia; [tlatov@mail.ru](mailto:tlatov@mail.ru)  
Received 2009 May 23; accepted 2010 March 19; published 2010 April 14

### ABSTRACT

We have analyzed the shape of the solar corona using the data of daily observations with Mark-III/IV (1980–2008) and *SOHO*/LASCO-2 (1996–2009) telescopes. The angles of deviation of coronal rays from the radial direction  $\Delta\theta$  vary cyclically, reaching the maximum deviation toward the solar equator at the minimum of the solar activity. We consider the relations between the angles of deviation of coronal rays and the parameters of the heliospheric current sheet, and discuss the hypothesis according to which the variations of the inclination  $\Delta\theta$  of coronal rays can affect the parameters of the solar wind and the indices of geomagnetic perturbations at the minima of the solar activity cycles.

*Key words:* interplanetary medium – solar wind – Sun: activity – Sun: corona – Sun: magnetic topology

### 1. INTRODUCTION

The coronal rays are distinctive structures in the solar corona, which propagate at a small angle to the radial direction from the Sun and display the electron density in K-corona enhanced by a factor of 3–10. They appear at ( $\sim 1.15$ – $2$ ) $R_o$  and are traced up to the distance above  $10 R_o$  (Bohlin 1970a, 1970b; Newkirk 1967). The angle  $\Delta\theta$  that describes the deviation of the rays from the radial position varies with the phase of the solar cycle (Kim et al. 2004) and the latitude (Eselevich & Eselevich 2002).

The awareness of the variations of the angle  $\Delta\theta$  with the phase of a cycle is important for theoretical models describing the structure of the corona and the geometry of the magnetic field above the solar limb (Wang 1996). The applied aspect of the studies for the deviations of coronal streamers, along with the plasma flows in the solar wind, is also of great importance, since the deviation may affect the geoefficiency of the solar wind impact (Pudovkin & Chertkov 1976).

When analyzing observations of total solar eclipses, a close in meaning parameter of the “flatness” of the shape of the corona is used, which also indicates the variation with the phase of the solar cycle (Vsekhsvyatsky et al. 1965).

Here, we present a comparative analysis for the deviation  $\Delta\theta$  of the propagation of coronal rays from radial propagation during several cycles of solar activity.

### 2. THE DATA

The regular observations with the *Solar and Heliospheric Observatory (SOHO)*/LASCO and Mark-III/IV coronagraphs at the Mauna Loa Solar Observatory make it possible to analyze the structure of the solar corona for the time comparable with the duration of the solar cycle. These data substantially complement extended series of observations of the corona in spectral lines carried out with extra-eclipse coronagraphs, since they make it possible to analyze coronal structures at sufficiently large distances from the solar limb, and also occasional observations of the “white light” corona during total eclipses. The coronagraph–polarimeter Mark-III detected the structure of the solar corona at the heights  $\sim 1.15$ – $2.45 R_o$  in 1980–1999. In 1998, at Mauna Loa Solar Observatory the new low-noise coronagraph Mark-IV, with a liquid-crystal modulator of polarization and a CCD, was mounted. To decrease the radial gradient and consequently to increase the contrast, we applied

to the Mark data an artificial vignetting function. The LASCO-2 coronagraphic telescope on board *SOHO* satellite has been working since 1996 and covers the distance  $1.5$ – $6 R_o$  above the solar limb. Thereby, here we have analyzed the structure of the corona for 1980–2008 on the basis of the data obtained at ground-based observations with Mark-III/IV coronagraphs and for 1996–2009 with the *SOHO*/LASCO-2 data.

### 3. THE IDENTIFICATION OF THE DEVIATION ANGLES OF CORONAL RAYS

In order to determine the deviation of coronal rays, we developed a technique for the identification of coronal streamers in two-dimensional images of the corona obtained with *SOHO*/LASCO-2 and Mark-III/IV in the automatic mode. The analysis is based on the discrimination of central parts of bright coronal structures propagating, as a rule, at some angle to the radial direction, the discrimination of the points of the local maxima, and the determination of the parameters of the approximating line section (Figure 1). The procedure included the following stages. Initially, the coordinates of the center and the radius of the Sun were measured in pixels. Further on, we calculated the average limb brightness of the corona for different heights above the solar limb  $I(r)$ . We considered the regions in which the brightness at a given distance from the limb was not smaller than  $0.3I(r)$ . Then we selected all the points corresponding to the local maximum within the segment, by the angle  $\pm 1^\circ 5'$  along the limb. The obtained collections of points, as a rule, represented regions close to the center of brightness of the coronal rays, extended from the limb of the Sun at some angle to the radial direction. For these regions, we inscribed the least-squares approximating straight lines. From the parameters of these straight lines, we determined the polar angle of the base of a coronal ray  $\theta$  and the deviation from the radial direction  $\Delta\theta$ . Figure 2 presents an example of such identification for a *SOHO*/LASCO-2 image obtained on 2007 March 16. We used for the analysis the deviation angle for these straight lines with respect to the radial propagation. We took into account line sections with the length not smaller than  $1.0R$  for *SOHO*/LASCO-2 images and than  $0.5R$  for Mark-III/IV images. The selection of rays, the linearity of which can be traced to a fairly large distance, allows us to filter out a considerable number of coronal structures associated with eruptive processes.

Thereby, we have processed about  $4.2 \times 10^3$  images for the time interval 1996–2009 and discriminated approximately  $10^5$

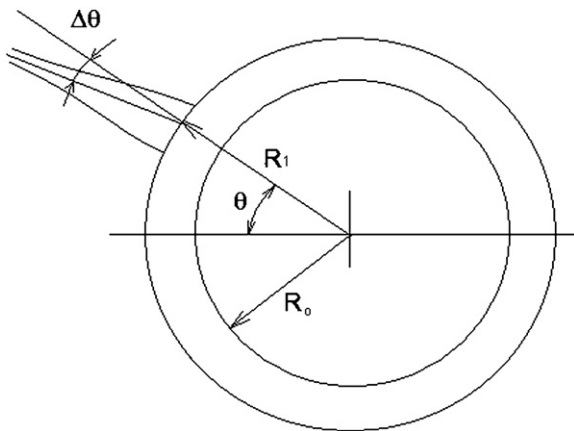


Figure 1. Determination of deviation angles for coronal rays.



Figure 2. Example of the identification of the direction of the propagation of coronal streamers for an image of the corona obtained with *SOHO/LASCO-2* on 2007 March 16.

coronal rays from the *SOHO/LASCO-2* data and  $7 \times 10^3$  days for the Mark-III/IV data for 1980–2008.

In this analysis, we recorded coronal beams of various types, including helmet-type rays, chains of streamers, and rays

belonging to the low-latitude and polar regions (Saito et al. 2000; Eselevich & Eselevich 2002). These rays can be formed over the bipolar and unipolar magnetic structures. There are also dynamic coronal rays, but we decided that their number should be small enough not to affect the comparison. Thus, Figure 3 shows that the footpoints of rays are usually evident in a few days. In addition to the geometry of the rays in the process of selection, we also recorded the absolute and relative brightness of the rays. This allowed us to make a comparative analysis of non-radial rays and define their types. In order to define the brightness of rays, we calculated the average intensity within the function from the height over the solar limb  $I_{avr}(r) = 1/2\pi \int_0^{2\pi} I_{avr}(r, \alpha) d\alpha$ , where  $\alpha$  is the polar angle. Then we defined the average intensity of a ray at the beginning and end of a segment, approximating the ray  $\bar{I} = (I_{beg} + I_{end})/2$ . The rays with the intensity  $\bar{I} > 2I_{avr}$ , where  $I_{avr}$  was calculated at a height  $(R_{end} + R_{beg})/2$ , were related to bright rays. The rays with the intensity  $\bar{I} < 1.3I_{avr}$  were conditionally related to non-bright rays. Figure 2 shows the systems of bright rays that are marked with numbers 1–3. The rays of lower intensity are normally located within the area of high latitudes (marked with number 4, Figure 2).

Footpoints of bright coronal rays, obtained under the assumption of a linear distribution, as a rule, are close to the neutral line (Figure 3(a)). Footpoints of coronal rays of low intensity are usually found in the areas of a large-scale unipolar field (Figure 3(b)).

Figure 4 shows the change of non-radial parameter for bright rays ( $\Delta\theta_{br}$ ) associated with helmet rays and soft rays ( $\Delta\theta_{low}$ ), which are typical for the chain of coronal streamers from the unipolar regions. Rays of varying brightness show a close cyclical course of the parameter  $\Delta\theta$ , although the degree of non-radiality for bright rays is slightly less:  $\Delta\theta_{br} = 1.46 + 0.47\Delta\theta_{low}$ , and are correlated with  $r = 0.79$ . Rays of different latitudinal zones also show a close behavior (Figure 5). The relationship between the parameters  $\Delta\theta$  for rays of the equatorial and polar zones is the following:  $\Delta\theta_{pol} = 4.1 + 0.84\Delta\theta_{eq}$ ;  $r = 0.89$ . Thus, the non-radial parameter  $\Delta\theta$  cycle exists for various types of coronal rays.

#### 4. THE RESULTS

The analysis of the *SOHO/LASCO-2* data for 1996–2009 indicates that the deviation angle  $\Delta\theta$  varies with the 11-year cycle of the activity, reaching the maximum values at the

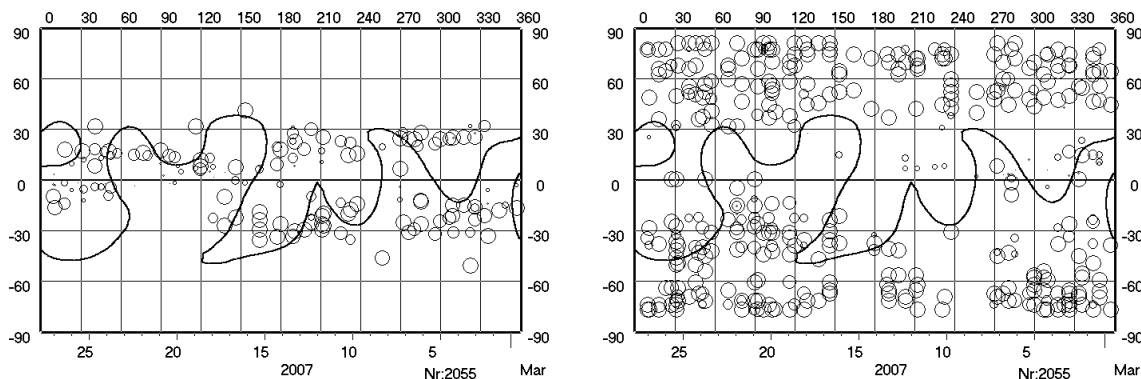
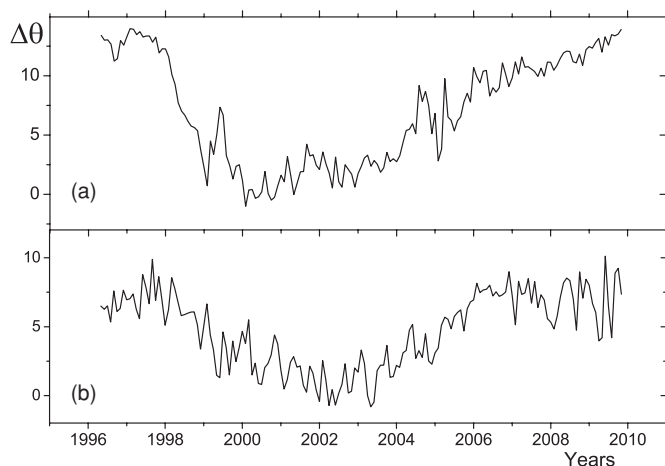
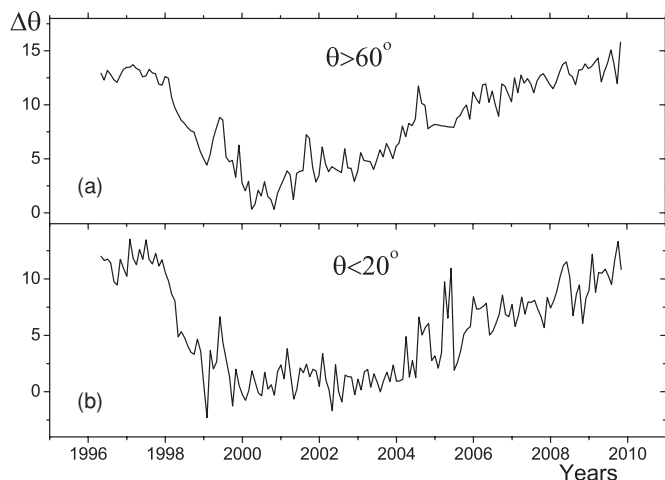


Figure 3. Example of synoptic maps for Carrington rotation N2055 which marked the neutral line, calculated at an altitude  $R = 1.9R_o$  according to the Wilcox Solar Observatory. Left: the footpoints of bright coronal rays ( $I > 2I_{avr}$ ). Right: the footpoints for coronal rays of low intensity ( $I < 1.3I_{avr}$ ). Data are shown according to the coronagraph *SOHO/LASCO-2*.



**Figure 4.** Monthly averaged deviation from the radial direction  $\Delta\theta$  derived from the *SOHO/LASCO-2* data (a) for coronal rays of low intensity ( $I < 1.3I_{avr}$ ) and (b) for bright coronal rays ( $I > 2I_{avr}$ ).



**Figure 5.** Monthly averaged deviation from the radial direction  $\Delta\theta$  derived from the *SOHO/LASCO-2* data (a) for the polar rays and (b) for the rays of the equatorial zone.

minimum of the activity. Figure 6 presents the time–latitude diagram for  $\Delta\theta$  variations. In the vicinity of the equator, the deviation of the rays from the radial direction reaches the minimum. Negative angles were seen in the northern hemisphere in 2002–2004 and in the southern hemisphere in 2000–2003, at the latitudes smaller than  $30^\circ$ . The coronal rays at the minimum of the activity and the phases of the decline are, as a rule, turned toward the solar equator. Only rather low-latitude coronal rays at the maximum of the activity slightly deviate toward the poles (Figure 6). The largest deviation from the radial direction is seen at the minimum of the activity at the latitudes  $30^\circ$ – $60^\circ$ . At the time of the maximum of the activity and the polarity reversal of the solar magnetic field, the rays are directed either parallel to the equator or slightly deviated toward the poles. Individual fluctuations of the angles of deviation of the rays are seen in different latitude zones (Figure 5), which indicate the general type of the perturbations of coronal structures.

Figure 7 presents the monthly averages for the deviation, averaged along the entire limb for all types of coronal rays. For comparison, the graph also shows the variation of the tilt angle  $\tau$  of the heliospheric current sheet (HCS; Hoeksema & Scherrer 1986). The tilt angle of HCS is calculated in a potential assumption of this photospheric magnetic field for

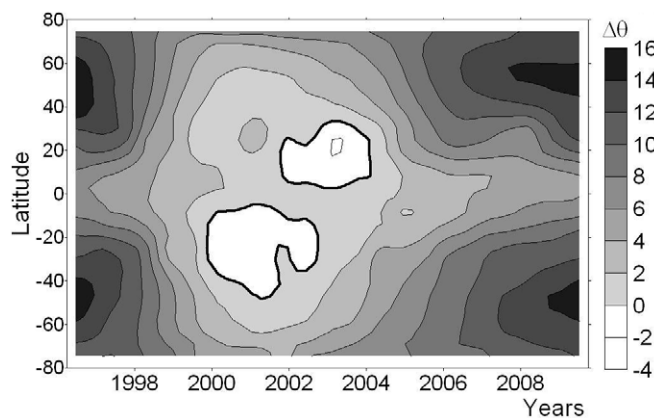


**Figure 6.** Latitude and time distribution of the angles of the deviation of coronal rays from the radial direction in the time interval 1996–2009 derived from the *SOHO/LASCO-2* data. The regions of the deviation of the rays toward the equator are darkened. The levels are indicated at the intervals of 2 deg; the level corresponding to  $\Delta\theta = 0^\circ$  is shown by the thick line.

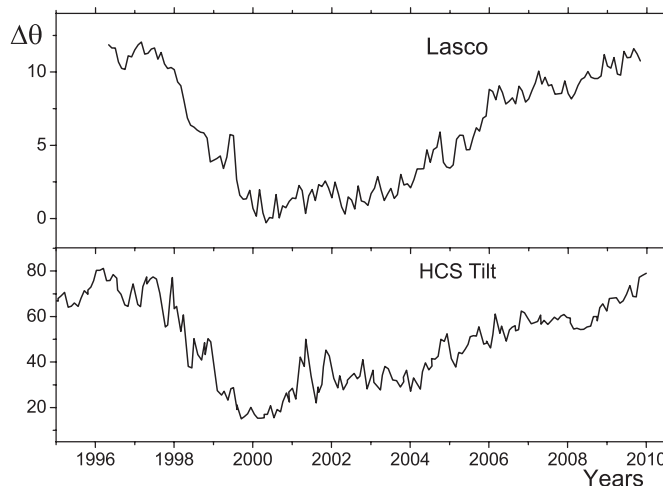


**Figure 7.** Comparison between the deviation  $\Delta\theta$  of coronal rays from *SOHO/LASCO-2* (top panel) and the inverted tilt angle of the heliospheric current sheet according to WSO (<http://wso.stanford.edu>).

$R = 3.25 R_\odot$ . Between these parameters there is the ratio  $\Delta\theta = 0.49 + 0.2\tau$ ;  $r = 0.91$ .

These conclusions are also confirmed by the analysis of the structure of the solar corona at the heights  $1.2$ – $2.5R$  based on the MLSO Mark-III/IV data. Figure 8 presents the angle  $\Delta\theta$  for the latitude zone  $\pm 30^\circ$  in the time interval 1980–2008. For the period 1996–2008, the angle  $\Delta\theta$  according to the coronagraph Mark was slightly lower than that according to LASCO/C2:  $\Delta\theta_{\text{Mark}} = 2.55 + 0.66\Delta\theta_{\text{LASCO}}$ ;  $r = 0.95$ . The non-radial variation  $\Delta\theta$  according to the Mark telescope during the 1980–2008 change of the parameter also has a good correlation with the tilt angle of HCS  $r \sim 0.8$  (Figure 8).

Figure 9 presents the latitude distribution for the  $\Delta\theta$  angle for the time of the minimum of the 23rd cycle. The maximum deviation is seen at the latitudes  $\sim 40^\circ$ – $50^\circ$ , which corresponds to the data obtained with the LASCO telescope (Eselevich & Eselevich 2002).

## 5. DISCUSSION

The deviation of coronal rays from the radial direction  $\Delta\theta$  related to the solar activity cycle may substantially affect the formation of the solar wind and geomagnetic perturbations.

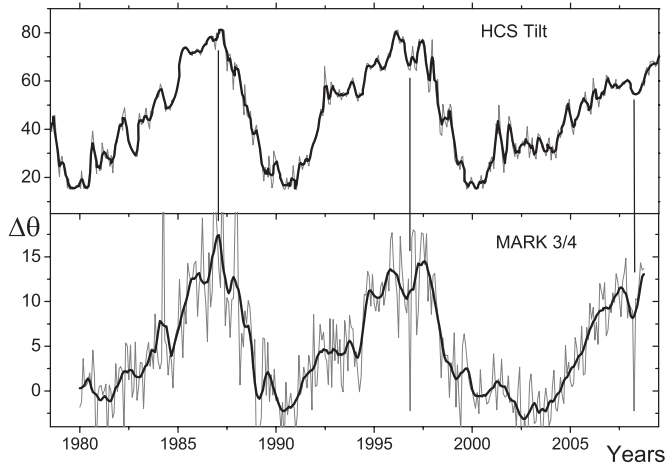


**Figure 8.** Comparison between the deviations  $\Delta\theta$  of coronal rays located in the middle-latitude zone  $\pm 30^\circ$  from the MLSO- MarkIII/IV data (bottom panel) and the inverted tilt angle of the heliospheric current sheet according to the WSO (top panel). The values are smoothed for 6 months.

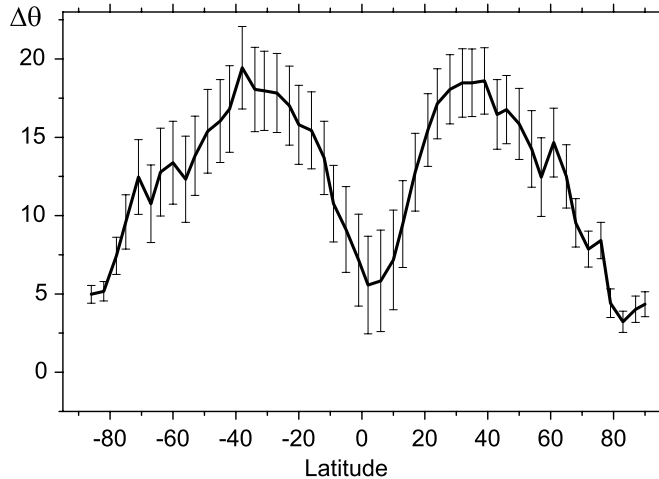


**Figure 9.** Variations of the angle  $\Delta\theta$  as a function of the latitude, obtained from the MLSO- Mark-III data at the minimum of the 23rd cycle of the solar activity (1996–1997).

From geometrical consideration, in Figure 1 the flux of the solar wind at the distance  $r$  is related to that at the distance  $R_1$ , where the current lines become straight, as follows:  $nv/n_1v_1 = 1 + (\theta - \Delta\theta) \cdot (r - R_1)/\theta \cdot R_1$ , for  $\Delta\theta < \theta$ . Assuming that at the years of the minimum activity  $\theta = 40^\circ$  and  $\Delta\theta = 20^\circ$  (Figure 9), we obtain that the ratio  $nv/n_1v_1$  at the distance 1 AU increases roughly twice compared to the case of radial expansion.

Figure 10 presents the graph of the deviation angle in comparison with the indices connected with parameters of a solar wind. In the years of the maximum activity, the influence of active regions and flares is substantial. However, during the years of minimum activity, the deviation  $\Delta\theta$  increases. The flow of solar wind is compressed to the plane of the solar equator and decreases the relative rate of expansion of the flow with distance from the Sun. The magnetic field acts as a nozzle. This can be one of the reasons for the delay of a solar wind (SW) speed (Figure 10(c)), and to modulate indices of geomagnetic activity  $aa$  (Figure 10(d)) and cosmic rays intensity (CRI) (Figure 10(b)).

The deviation coronal streamers  $\Delta\theta$  occur as the cyclic process appreciable at all solar latitudes (Figures 5 and 6). Probably, it is connected with global processes, for example, hemispheric current layer (Filippov 2009).

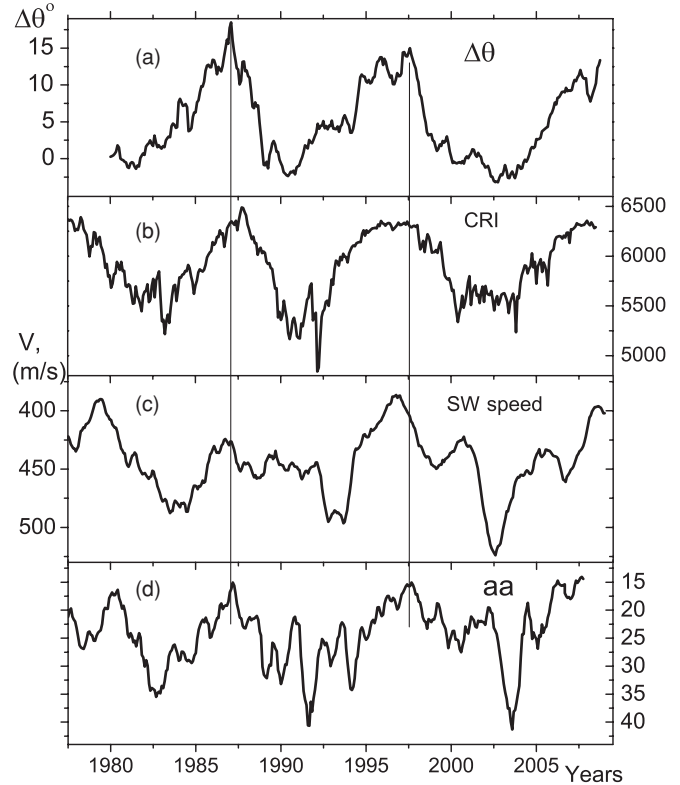


**Figure 10.** Comparison between (a) the deviations of coronal rays  $\Delta\theta$ ; (b) data of Kiel cosmic-ray intensity (arbitrary units, monthly means); (c) speed of the solar wind according to OMNI2 database was smoothed on 20 Bartels rotations; (d) the geomagnetic index  $aa$ , the data are smoothed with a sliding window technique for 6 months.

In the analysis we have considered various structures, including possibly producing a unipolar coronal streamer belt called “chains of streamers” or “streamer belt without a neutral line” by Eselevich et al. (1999) as well as the bipolar streamer belt (Zhao & Webb 2003). These streamers vary in brightness and location of footpoint. Our analysis of separation of their brightness and latitude showed that cyclic changes in the non-radial parameter  $\Delta\theta$  exist for various types of coronal streamers. The good agreement between the change in time for parameter  $\Delta\theta$  and the change in the angle of inclination of HCS suggests that the parameter of non-radiality is possibly conditioned by the existence of current in the heliospheric current layer. The current in the HCS can be estimated from the parameter  $\Delta\theta$ .

Thereby, we may suggest a link between the large-scale magnetic field and the deviation of coronal rays toward the equator, which in turn affects the level of geomagnetic indices at a solar minimum as well as solar–terrestrial relations.

The work was supported by the Russian Foundation for Basic Research (RFBR), the Russian Academy of Sciences, and the Program to Support Leading Scientific Schools by the Russian Federal Agency for Science and Innovations (NS-3645.2010.2)

I am also indebted to K. Maslenikov for his assistance in preparing the English version of the manuscript.

## REFERENCES

- Bohlin, J. D. 1970a, *Sol. Phys.*, **12**, 240  
Bohlin, J. D. 1970b, *Sol. Phys.*, **13**, 153

- Eselevich, V. G., & Eselevich, M. V. 2002, *Sol. Phys.*, **208**, 5
- Eselevich, V. G., Fainshtein, V. G., & Rudenko, G. V. 1999, *Sol. Phys.*, **188**, 277
- Filippov, B. P. 2009, *Astron. Rep.*, **53**, 564
- Hoeksema, J. T., & Scherrer, P. H. 1986, *Sol. Phys.*, **105**, 205
- Kim, G-D., Makarov, V. I., & Tlatov, A. G. 2004, *Int. J. Geomagn. Aeronomy*, **5**, G12011
- Newkirk, G. 1967, *ARA&A*, **5**, 213
- Pudovkin, M. I., & Chertkov, A. D. 1976, *Sol. Phys.*, **50**, 213
- Saito, T., Shibata, K., Dere, K. P., & Numazawa, S. 2000, *Adv. Space Res.*, **26**, 807
- Vsekhsvyatsky, S. K., Nikolsky, G. M., Ivanchuk, V. I., Nesmuanovich, A. T., Ponomarev, E. A., Rubo, G. A., & Cherednichenko, V. I. 1965, *The Solar Corona and Corpuscular Emission in Interplanetary Space* (Kiev: Kiev Univ. Press), 293
- Wang, Y.-M. 1996, *ApJ*, **456**, L119
- Zhao, X. P., & Webb, D. F. 2003, *J. Geophys. Res.*, **108**, 1234